Quaternary Research

doi:10.1017/qua.2019.83

Radiocarbon simulation fails to support the temporal synchroneity requirement of the Younger Dryas impact hypothesis

Ian A. Jorgeson[a], Ryan P. Breslawski[a]*, Abigail E. Fisher[a]

[a]Department of Anthropology, Southern Methodist University, P.O. Box 750235, Dallas, Texas 75275, USA
*Corresponding author e-mail address: rbreslawski@smu.edu (R.P. Breslawski).

(Received July 29, 2019; Accepted December 9, 2019)

Abstract

Fine-scale temporal processes, such as the synchronous deposition of organic materials, can be challenging to identify using ^{14}C datasets. While some events, such as volcanic eruptions, leave clear evidence for synchronous deposition, synchroneity is more difficult to establish for other types of events. This has been a source of controversy regarding ^{14}C dates associated with a hypothesized extraterrestrial impact at the Younger Dryas Boundary (YDB). To address this controversy, we first aggregate ^{14}C measurements from Northern Hemisphere YDB sites. We also aggregate ^{14}C measurements associated with a known synchronous event, the Laacher See volcanic eruption. We then use a Monte Carlo simulation to evaluate the magnitude of variability expected in a ^{14}C dataset associated with a synchronous event. The simulation accounts for measurement error, calibration uncertainty, "old wood" effects, and laboratory measurement biases. The Laacher See ^{14}C dataset is consistent with expectations of synchroneity generated by the simulation. However, the YDB ^{14}C dataset is inconsistent with the simulated expectations for synchroneity. These results suggest that a central requirement of the Younger Dryas Impact Hypothesis, synchronous global deposition of a YDB layer, is extremely unlikely, calling into question the Younger Dryas Impact Hypothesis more generally.

Keywords: Radiocarbon dating; Monte Carlo simulation; Younger Dryas Impact Hypothesis; Laacher See Tephra; late Quaternary; Terminal Pleistocene

INTRODUCTION

Resolving temporal questions at decadal or annual scales using radiocarbon (^{14}C) dates is difficult (Bronk Ramsey, 2008). This is especially true of cases in which researchers attempt to distinguish a synchronous event from an asynchronous process that occurred over multiple years or decades. Here, we consider two ^{14}C datasets relevant to this problem: ^{14}C measurements associated with the Laacher See volcanic eruption in Germany (Baales et al., 2002) and ^{14}C measurements associated with the hypothesized Younger Dryas extraterrestrial impact, recovered from contexts in Asia, Europe, and North America (Fig. 1; Kennett et al., 2015). In principle, calibrated ^{14}C measurements of organic material associated with each event or hypothesized event should be tightly clustered around a value corresponding to the calendar year of that event. However, in practice, multiple sources of uncertainty may cause ^{14}C measurements to be more dispersed than expected, obscuring the difference between a synchronous depositional event and a depositional process that occurred over multiple decades or centuries (Baillie, 1991).

Sources of uncertainty include imprecision in the measurement of ^{14}C, captured in reported measurement errors, and in the calibration of those measurements into calendar years (Bronk Ramsey, 2008). The ^{14}C measurement and calibration process produces continuous non-normal, often multimodal, calendar date distributions with high probability regions that can span multiple centuries (Bronk Ramsey, 2009a). Additional uncertainty can arise from chronological mismatches between the death and deposition of sample organisms, often referred to as "old wood" effects (Dean, 1978; Schiffer, 1986; Bronk Ramsey, 2009b), as well as systematic biases in laboratory measurements and variability in measurement repeatability between laboratories (Polach, 1974; International Study Group, 1982; Scott et al., 1990, 1998, 2007, 2010a, 2010b Boaretto et al., 2003; Christen and Pérez, 2009). The direction and magnitude of these sources of

Cite this article: Jorgeson, I. A., Breslawski, R. P., Fisher, A. E. 2020. Radiocarbon simulation fails to support the temporal synchroneity requirement of the Younger Dryas impact hypothesis. *Quaternary Research* 96, 123–139. https://doi.org/10.1017/qua.2019.83

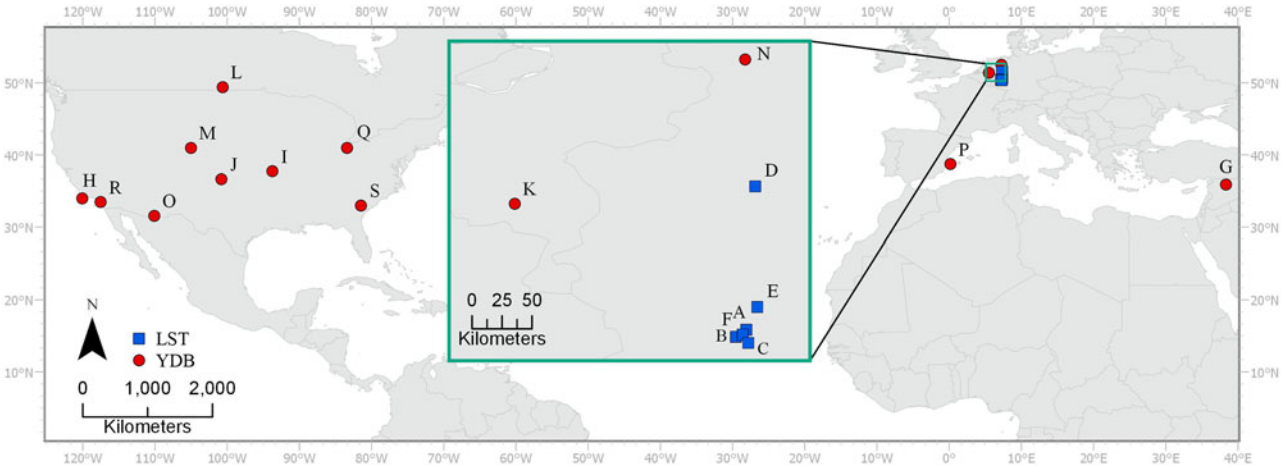

Figure 1. Map of Laacher See Tephra (LST) and Younger Dryas Boundary (YDB) localities. Inset map (green border) shows detailed view of localities in northern Europe. Alphabetic site IDs are listed in Table 1. (For interpretation of the references to color in this figure legend, the reader is referred to the web version of this article.)

uncertainty are not constant, varying from one set of ^{14}C measurements to another.

Existing statistical methods for evaluating synchroneity in ^{14}C datasets do not fully account for these context-dependent uncertainties. One such method applies a χ^2 test to a series of ^{14}C measurements under the null hypothesis that the ^{14}C measurements are of the same calendar age (Ward and Wilson, 1978). However, when this approach is applied to complex synchronous ^{14}C datasets with many sources of uncertainty, it can generate large χ^2 test statistics with low P values, and so falsely reject synchroneity. A more recent approach to determining whether two dates could be synchronous involves calculating the distribution of temporal distances between both calibrated age densities (Parnell et al., 2008; see also, the Difference command in the Oxcal ^{14}C calibration software [Bronk Ramsey, 2008]). If the 95% highest density interval of this distribution includes zero (i.e., there is some overlap in the calibrated age densities at the 95% threshold), synchroneity is considered plausible and therefore not rejected. However, this approach cannot estimate the probability of obtaining the observed age densities, given a synchronous event, and thus does not distinguish between datasets that are unlikely to have been generated by a synchronous event and those that are more likely to have been deposited synchronously.

In this paper, we develop a simulation-based technique for assessing synchroneity that accounts for the sources of uncertainty specific to a given ^{14}C dataset. We apply this technique to the observed ^{14}C datasets associated with the Laacher See volcanic eruption and the hypothesized Younger Dryas extraterrestrial impact. Here, we define a "geologically synchronous event" as an event that deposited organic material within a one-year period.

Laacher See volcanic eruption and associated ^{14}C dataset

The Laacher See (Germany) volcanic eruption occurred ~12,900 cal yr BP (Schmincke et al., 1999; Baales et al., 2002). The volcano, located in western Germany, ~40 km south of the city of Bonn, consists of two craters linked by a single submerged vent (van den Bogaard and Schmincke, 1985; Baales et al., 2002). The Laacher See Tephra (LST) is concentrated in central Europe, with associated ash having been identified as far south as Italy, north to the Baltic Sea, west into France, and east into Poland (van den Bogaard and Schmincke, 1985; Schmincke et al., 1999). The LST is visible in three geochemically distinct stratigraphic layers representing three eruptive phases: the Lower, Middle, and Upper LST. Combined, these three layers form a tephra that exceeds 50 m thick near the volcanic vent, decreasing to ~10 m thick at four km from the vent (Schmincke et al., 1999).

The bulk of volcanic activity likely occurred over a span of ~10 hours, with complete deposition of the three associated LST layers within a period of several months (Schmincke et al., 1999). Given that deposition of the combined Lower, Middle, and Upper LST occurred within a single calendar year (van den Bogaard, 1983; van den Bogaard and Schmincke, 1985; Park and Schmincke, 1997; Schmincke et al., 1999), the Laacher See volcanic eruption meets our definition for a geologically synchronous event. We thus treat ^{14}C samples from any of the three layers as originating from the same event (*sensu* Baales et al., 2002).

We identified 19 previously published ^{14}C measurements on samples collected from within the Lower, Middle, or Upper LST at six German localities (Fig. 2, Table 1). All but one measurement (HV-11774, short lived plant remains) are on wood samples, primarily trees of the genus *Populus*, and none of them are accelerator mass spectrometer (AMS) measurements. We excluded three LST ^{14}C measurements from Kruft that correspond to three sequential sets of rings from one tree specimen, *Populus* 9 (measurements HD-19092, HD-18622, and HD-19037), and only included the measurement taken on the outermost available *Populus* 9 rings, HD-19098, corresponding to the ^{14}C measurement for a date closest to the deposition of the LST. These 19 ^{14}C measurements constitute the observed LST dataset (LST_{Obs}).

https://doi.org/10.1017/qua.2019.83 Published online by Cambridge University Press

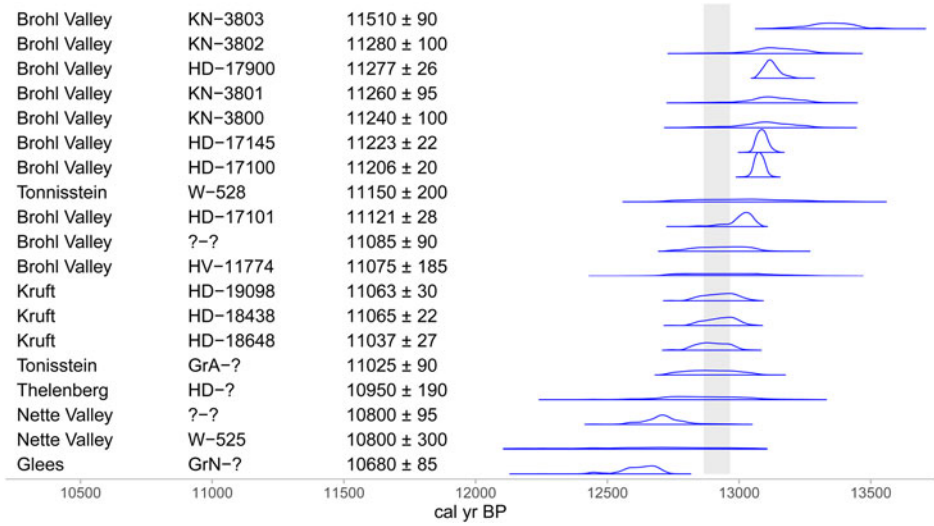

Figure 2. Calibrated age densities for samples originating from LST contexts (LST_{Obs}). The right column of text displays the means and standard errors for each sample in ^{14}C yr BP. Light blue distributions show dates obtained through gas proportional or liquid scintillation counting. Open densities correspond to dates with potential "old wood" effects (all samples other than HV-11774). The grey band marks the range of possible years for the Laacher See volcanic eruption, 12,966–12,866 cal yr BP. Question marks denote samples for which original sources did not report laboratory sample IDs. See Table 1 for references. (For interpretation of the references to color in this figure legend, the reader is referred to the web version of this article.)

Previous research with ^{14}C dates, lake varve records, and tree-ring chronologies suggests a most likely calendar date of 12,916 cal yr BP for the deposition of the LST (Baales et al., 2002). Given that the true date is imprecisely known, we consider a 101-yr window centered on this date (12,966 to 12,866 cal yr BP).

The Younger Dryas Boundary (YDB) and associated ^{14}C dataset

The Younger Dryas Impact Hypothesis posits that an extraterrestrial body collided with North America, most likely on some date between 12,835 and 12,735 cal yr BP (Kennett

Table 1. Laacher See Tephra and Younger Dryas Boundary localities with number (n) of ^{14}C measurements. Alphabetic ID corresponds to site locations in Figure 1.

	ID	Locality	*n*	References
Laacher See	A	Brohl Valley	10	Frechen, 1952; Schweitzer, 1958; Heine, 1993; Street, 1993; Kromer et al., 1998
	B	Glees	1	Schweitzer, 1958
	C	Kruft	3	Baales et al., 1998
	D	Nette Valley	2	Frechen, 1959; van den Bogaard and Schmincke, 1985
	E	Thelenberg	1	Frechen, 1959
	F	Tönisstein	2	Frechen, 1959; Rubin and Alexander, 1960; Street et al., 1994
Younger Dryas Boundary	G	Abu Hureyra	1	Wittke et al., 2013
	H	Arlington Canyon	12	Kennett et al., 2008
	I	Big Eddy	2	Lopinot et al., 1998; Hajic et al., 2007
	J	Bull Creek	1	Bement et al., 2014
	K	Geldrop-Aalsterhut	3	van Hoesel et al., 2012
	L	Lake Hind	1	Firestone et al., 2007
	M	Lindenmeier	1	Haynes and Agogino, 1960; Walton et al., 1961
	N	Lingen	1	Kennett et al., 2015
	O	Murray Springs	2	Haynes, 2007
	P	Santa Maira	1	Aura Tortosa et al., 2008
	Q	Sheridan Cave	3	Tankersley and Redmond, 1999; Waters et al., 2009
	R	Talega	1	Bergin, 2011; Wittke et al., 2013
	S	Topper	1	Goodyear, 2013

https://doi.org/10.1017/qua.2019.83 Published online by Cambridge University Press

et al., 2015), causing widespread burning, megafaunal extinctions, the onset of Younger Dryas cooling, and the disappearance of the Clovis archaeological culture (Firestone et al., 2007; Kennett et al., 2008, 2015; Firestone, 2009; Wolbach et al., 2018a, 2018b). Supporters of the hypothesis argue that this event is recognizable in the Younger Dryas Boundary (YDB) stratum at sites in North and South America, Europe, and Asia based on the presence of impact proxies such as nanodiamonds, carbon spherules, magnetic spherules, and increased platinum (Firestone et al., 2007; Kennett et al., 2008, 2009a, 2009b, 2015; Firestone, 2009; Israde-Alcantara et al., 2012; Bunch et al., 2012; LeCompte et al., 2012; Petaev et al., 2013; Wittke et al., 2013; Wu et al., 2013; Kinzie et al., 2014; Moore et al., 2017; Kletetschka et al., 2018; Pino et al., 2019). However, independent researchers have failed to identify the proposed impact proxies in YDB aged sediments (Surovell et al., 2009; Daulton et al., 2010, 2017; Haynes et al., 2010; Holliday et al., 2016), questioned whether the markers are necessarily the result of an impact (van der Hammen and van Geel, 2008; A.C. Scott et al., 2010; Pigati et al., 2012; van Hoesel et al., 2012), criticized the methodologies used to date layers containing impact markers (Holliday and Meltzer, 2010; Blaauw et al., 2012; Meltzer et al., 2014; van Hoesel et al., 2014), or disputed the plausibility of an impact or airburst as described by proponents (Boslough et al., 2012). Proponents have also recently proposed that the hypothesized event produced the Hiawatha impact crater located in Greenland (Pino et al., 2019). However, the age of this crater remains unknown, with constraints suggesting only that it was formed some time during the Pleistocene (~11,000–2,588,000 cal yr BP; Kjær et al., 2018).

We collated measurements specified by Kennett et al. (2015) as originating from a YDB layer containing impact markers. Kennett et al. (2015) identified YDB layers at 23 sites in North and South America, Europe, and Asia. Earlier iterations of the Younger Dryas Impact Hypothesis included additional sites, such as Wally's Beach, Howard Bay, Myrtle Beach, and Lumberton (Firestone et al., 2007; Firestone, 2009). However, other researchers were unable to confirm the presence of impact markers (Paquay et al., 2009) or questioned the age of these sites (Pinter et al., 2011; Meltzer et al., 2014), and proponents of the hypothesis have since dropped them from consideration. Of the 23 sites presented in Kennett et al. (2015), 13 have ^{14}C samples taken directly from the YDB. In total, Kennett et al. (Kennett et al., 2015) identified 32 YDB ^{14}C samples from these 13 sites.

We considered those 32 ^{14}C samples presented by Kennett et al. (2015) as originating from the YDB. However, we subsequently excluded two of these samples: AA-25778 from Big Eddy (10,260 ± 85 ^{14}C yr BP) and TX-1044 from Murray Springs (12,600 ± 2440 ^{14}C yr BP). We excluded AA-25778 since it was flagged as an outlier in Kennett et al.'s (2015) age-depth model and TX-1044 due to its anomalously large measurement error. This left 30 ^{14}C measurements in the observed YDB ^{14}C dataset (YDB_{Obs}; ×Fig. 3, Table 1). All but three of the 30 ^{14}C measurements in YDB_{Obs} are AMS (A-1045, TX-1045, and I-141). Most of these measurements are charcoal samples ($n = 17$), although wood ($n = 7$), soil organic matter (SOM; $n = 2$), bone ($n = 1$), and carbon elongate/spherule ($n = 3$) samples are also present. As Kennett et al. (2015) proposed a likely calendar age for the hypothesized impact between 12,835 and 12,735 cal yr BP, we consider the 101 calendar yr in this range.

Supplementary data details the LST_{Obs} and YDB_{Obs} ^{14}C samples, including additional ^{14}C samples that we excluded due to unclear or disputed spatial association with either stratum.

METHODS

Monte Carlo simulation

We developed a Monte Carlo simulation that generates a distribution of expected sets of ^{14}C measurements, given a geologically synchronous event. Terms relevant to the simulation are defined in Table 2. These simulated expected datasets are referred to here as LST_{Sim} and YDB_{Sim}. For a given calendar year, the simulation first replicates that year n times, where n is the number of samples in the observed dataset. The simulation uses the IntCal13 (Reimer et al., 2013) calibration curve to uncalibrate each of the n calendar years to produce simulated ^{14}C measurements, and then recalibrates the ^{14}C measurements into calendar ages. During this process, offsets are applied to the simulated values, representing sources of uncertainty specific to the observed dataset (Table 3). Some offsets, representing uncertainty in the difference between the time of organism death and the time of deposition, are applied to the n calendar years before they are uncalibrated. Other offsets, representing uncertainty in the measurement of ^{14}C, are applied between uncalibration and recalibration. Uncertainty in the concentration of atmospheric ^{14}C is accounted for by recalibration. One iteration of the simulation thus produces a set of n ^{14}C measurements with associated calibrated ages. This repeats for 10,000 iterations per calendar year of interest, generating a distribution of simulated datasets that can be compared against the observed dataset. If the observed measurements (LST_{Obs} and YDB_{Obs}) are substantially less clustered (more dispersed) than those in the simulated distribution of datasets (LST_{Sim} and YDB_{Sim}), we conclude that the observed dataset is inconsistent with a synchronous event, and thus more consistent with deposition over multiple years. In contrast, if the observed measurements are as or more clustered (less dispersed) than those in the simulated distribution of datasets, we conclude that the observed dataset is consistent with a synchronous event.

We measure clustering in ^{14}C datasets with two metrics: the standard deviation of ^{14}C measurements ($\sigma^{14}C$) and the dissimilarity between calibrated age densities (as measured by the mean pairwise Manhattan distance defined in Eq. 1). The Monte Carlo simulations are applied to two observed datasets: first, LST_{Obs}, a dataset produced by a known synchronous event, and hence a useful "control" for validating the simulation; and second, YDB_{Obs}.

https://doi.org/10.1017/qua.2019.83 Published online by Cambridge University Press

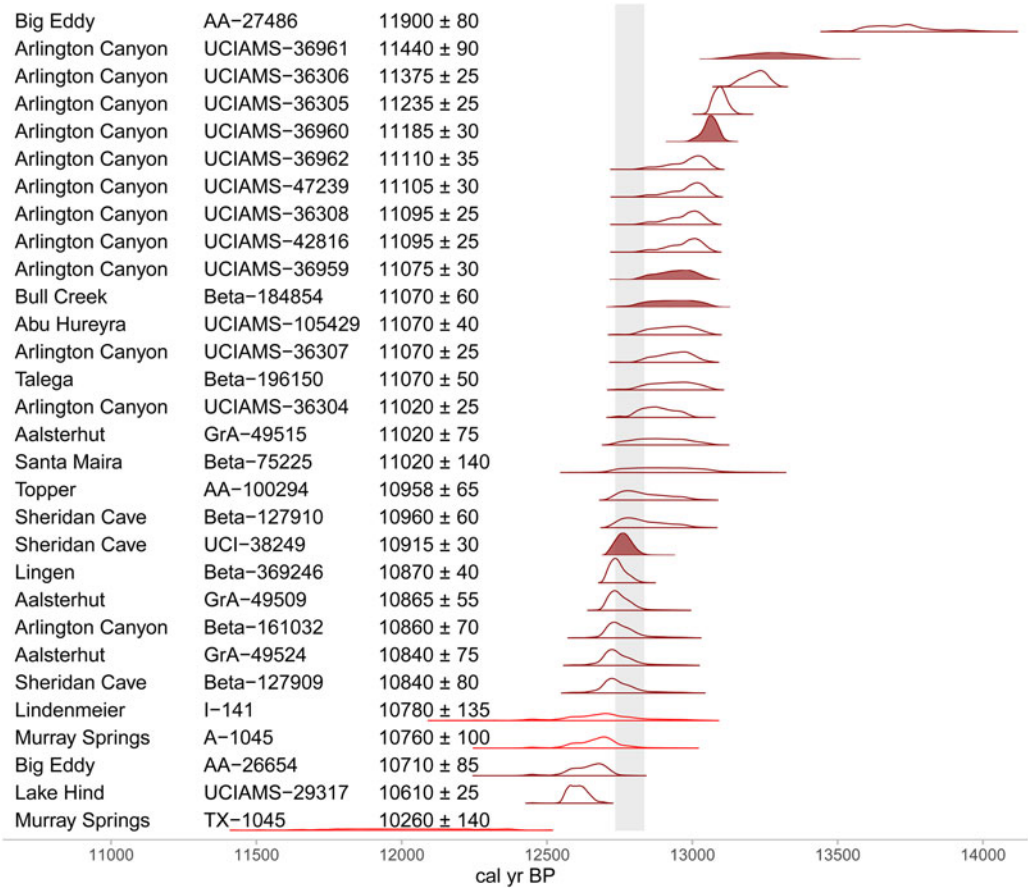

Figure 3. Calibrated age densities for samples originating from YDB contexts (YDB_{Obs}). The right column of text displays the means and standard errors for each sample in ^{14}C yr BP. Dark red distributions show accelerator mass spectrometry (AMS) dates and light red distributions show dates obtained through gas proportional or liquid scintillation counting. Open densities correspond to dates with potential "old wood" effects. The grey band marks the range of possible years for the hypothesized extraterrestrial impact, 12,835–12,735 cal yr BP. See Table 1 for references. (For interpretation of the references to color in this figure legend, the reader is referred to the web version of this article.)

For each possible year in the 101-yr span centered on each event, the Laacher See eruption and hypothesized Younger Dryas impact, we simulated 10,000 expected sets of ^{14}C measurements (LST_{Sim} and YDB_{Sim}). Each YDB_{Sim} contains 30 ^{14}C measurements, and each LST_{Sim} 19 ^{14}C measurements, corresponding to the number of measurements in each observed dataset. First, we generated 30 (or 19) calendar dates for the possible year. Then, x calendar dates were offset for "old wood" effects, where x is number of samples in the *observed* dataset that are wood or charcoal.

Offsets are handled by two alternative "old wood" models (OWM), each of which increases calendar ages for wood and charcoal samples by drawing random values from an exponential distribution: $\lambda = 0.04$ for the smaller offset OWM (mean expected offset = 25 yr, 95% of expected values within 0–75 yr) and $\lambda = 0.01$ for the larger offset OWM (mean expected offset = 100 yr, 95% of expected values within 0–300 yr). The number of years by which "old wood" dates are offset from the events of interest within YDB_{Obs} and LST_{Obs} may be unknowable, but we assume it falls somewhere between the smaller and larger offsets in the OWMs used here. As such, the OWMs are intended to bound extreme possibilities for "old wood" effects in each dataset. Next, all calendar dates are converted to *target* ^{14}C values by sampling from the error distribution of the IntCal13 ^{14}C calibration curve (Reimer et al., 2013) corresponding to those calendar dates. We also ran simulations that did not apply "old wood" effects.

In some simulations, we also considered laboratory variability in ^{14}C measurements with a laboratory bias and repeatability model (LBM). The LBM simulates between- and within-laboratory variability in ^{14}C measurements through a Bayesian multilevel model fitted to a dataset of 361 ^{14}C measurements on six sample materials, as measured independently by 68 laboratories in the Fifth International Radiocarbon Intercomparison (Scott et al., 2007, 2010a, 2010b). Systematic laboratory biases are randomly sampled from the between-laboratory variability parameters of the fitted LBM, with the number of sampled values corresponding to the number of laboratories that contributed to the observed dataset. Variation in measurement repeatability is simulated by randomly sampling from the within-laboratory variability parameters of the fitted model. The LBM also accounts for variation arising from ^{14}C measurement using gas proportional

https://doi.org/10.1017/qua.2019.83 Published online by Cambridge University Press

Table 2. Terms used in this paper.

Term	Definition
Target ^{14}C value	The ^{14}C value corresponding to the calendar year in which a sample organism died. In the simulation, these values are obtained by randomly sampling from the error distribution of the IntCal13 calibration curve specific to a given calendar year.
Measured ^{14}C value	The ^{14}C value specific to a given calendar year as *measured* by a laboratory. In the simulation, these values are obtained by adding random error to target ^{14}C values using the LBM.
YDB	Younger Dryas Boundary: the geologic marker horizon for the hypothesized Younger Dryas extraterrestrial impact.
LST	Laacher See Tephra: the geologic marker horizon for the Laacher See volcanic eruption.
$YDB_{Obs/Sim}$	Observed and simulated datasets of ^{14}C measurements associated with the YDB.
$LST_{Obs/Sim}$	Observed and simulated datasets of ^{14}C measurements associated with the LST.
$\sigma^{14}C$	The standard deviation of ^{14}C measurements in an observed or simulated dataset of ^{14}C measurements. Larger values indicate more dispersed ^{14}C measurement.
Dissimilarity	The amount of overlap between calibrated age densities in a simulated or observed dataset. It is the mean pairwise Manhattan distance (Eq. 1). Values closer to 1 indicate more dispersed ^{14}C measurements.
OWM	Old wood model: an exponential probability distribution that defines the expected age offsets for "old wood" target ^{14}C values in the simulation. We considered exponential distributions with the λ parameter (i.e., the rate parameter of the exponential distribution) set to 0.04 and 0.01. Smaller λ values produce larger simulated offsets on average.
LBM	Laboratory bias and repeatability model: a multilevel model that defines the amount of measurement variability expected around a target ^{14}C value, given within-laboratory and between-laboratory measurement error. This is integrated into the simulation. The LBM was fitted to ^{14}C measurements published for the Fifth International Radiocarbon Intercomparison (Scott et al., 2007; E.M. Scott et al., 2010a, 2010b).

counting (GPC), liquid scintillation counting (LSC), or AMS. Values measured using either GPC or LSC are more variable than are values measured with AMS (Scott et al., 2007, 2010a, 2010b), and this difference is reflected in offsets generated by the LBM. These randomly sampled values were then applied as offsets to the *target* ^{14}C values, yielding *measured* ^{14}C values.

The output of the LBM provides the simulated expected dataset (LST_{Sim} and YDB_{Sim}), consisting of a set of *measured* ^{14}C values obtained by multiple laboratories with varying degrees of systematic bias and measurement repeatability. For those simulations that do not use the LBM, the *target* ^{14}C values sampled from the calibration curve serve as the simulated dataset. The different combinations of OWM λ values and inclusion or exclusion of the LBM lead to six different simulation parameterizations (Table 3).

For each simulated ^{14}C dataset, two measures of clustering are calculated. First, the simulation computes $\sigma^{14}C$ for the raw measurements. Second, we calibrate the raw measurements with the IntCal13 calibration curve (Reimer et al., 2013) and compute a dissimilarity value for the calibrated age densities. We define dissimilarity as the mean pairwise Manhattan distance between these age densities,

$$\frac{\sum_{x=1}^{n}\sum_{y=1}^{n}\sum_{i=1}^{c}|A_{x,i}-A_{y,i}|}{2(n^2-n)}, \qquad \text{(Equation 1)}$$

where A is a set of n vectors of calibrated age densities, i is a calendar year in vector I of length c, and I is a vector of the union of calendar years across all calibrated age densities in A. The denominator includes a value of 2 so that dissimilarity values are scaled to [0–1], with values closer to zero indicating smaller average differences between pairs of calibrated ages, and thus more clustering.

In total, for every possible calendar year in each proposed 101-yr span, each of the six simulations generates a distribution of 10,000 $\sigma^{14}C$ and dissimilarity values from 10,000 simulated expected datasets. We then compare the distributions of the simulated $\sigma^{14}C$ and dissimilarity values to the $\sigma^{14}C$ and dissimilarity values for LST_{Obs} and YDB_{Obs}. These comparisons address whether the observed values are larger than the simulation indicates would be expected for a synchronous event. Different combinations of the OWMs and the LBM allow us to explore how different sources of variability influence the simulated distributions of clustering values. Repeating the simulations for multiple calendar years allows us to investigate how the shape of the ^{14}C calibration curve impacts the distributions of $\sigma^{14}C$ and dissimilarity values. All simulations model the effects of uncertainty in the ^{14}C calibration curve, inter- and intra-annual atmospheric ^{14}C variability, and the reported ^{14}C measurement errors in each observed dataset.

For the Laacher See Tephra, the LST_{Obs} $\sigma^{14}C$ value is 196.94 and the LST_{Obs} dissimilarity value is 0.71 (Table 4). Since the LST was deposited synchronously, we expect that our simulations of synchronous LST_{Sim} datasets will produce distributions of $\sigma^{14}C$ and dissimilarity values that are consistent with the LST_{Obs} values. If, however, LST_{Sim} values are consistently more clustered than LST_{Obs} values, this would indicate that the simulation is not fully accounting for important sources of variability in ^{14}C datasets.

For the Younger Dryas Boundary, if the 30 YDB_{Obs} ^{14}C measurements represent a synchronous event, then the

https://doi.org/10.1017/qua.2019.83 Published online by Cambridge University Press

Table 3. Parameters for each simulation.

	Old wood model (OWM) λ value		
	No OWM	λ = 0.04	λ = 0.01
No LBM	Simulation A1	Simulation B1	Simulation C1
Includes LBM	Simulation A2	Simulation B2	Simulation C2

observed $\sigma^{14}C$ (282.02) and dissimilarity (0.75) values should fall within high probability regions of the simulated $\sigma^{14}C$ and dissimilarity value distributions. If, however, simulated distributions consistently have values smaller than YDB_{Obs} values, indicating that YDB_{Sim} datasets are more tightly clustered than YDB_{Obs}, then it is unlikely that YDB_{Obs} represents a synchronous event.

The simulation was performed in R 3.5.1 (R Core Team, 2018) and relies on functions from the R packages *parallel* (R Core Team, 2018), *rcarbon* (Bevan and Crema, 2018), *ggplot2* (Wickham, 2016), *patchwork* (Pedersen, 2018), *rethinking* (McElreath, 2017), *rstan* (Stan Development Team, 2018), *reshape2* (Wickham, 2007), and *matrixStats* (Bengtsson et al., 2018). The R script and spreadsheets of ^{14}C measurements for this simulation are provided as supplementary data.

Alternative observed datasets

The simulated distributions of LST_{Sim} and YDB_{Sim} are contingent on features of LST_{Obs} and YDB_{Obs}, including the reported ^{14}C measurement errors, the number of "old wood" dates, the number of participating laboratories, and the type of ^{14}C dating method (AMS or GPC/LSC). Alternative observed datasets could produce simulated $\sigma^{14}C$ and dissimilarity value distributions that suggest that the observed datasets are either more or less consistent with expectations. This presents a potential problem, as variability in reasonable researcher decisions must correspond to variability in results. Due to this issue, we also include a limited "multiverse analysis" (Steegen et al., 2016), in which we detail the results of simulations with alternative datasets to illustrate the degree to which our findings vary with data inclusion decisions. Our multiverse analysis is "limited" because we cannot anticipate every possible argument that might be made for including or excluding certain measurements. We therefore analyzed three alternative LST_{Obs} and YDB_{Obs} specifications that we felt were most likely to arise from other researchers' decisions and repeated the six simulations for each of the three datasets.

Alternative 1 includes the five ^{14}C measurements that were excluded from YDB_{Obs} and LST_{Obs}: TX-1044 (12,600 ± 2440 ^{14}C yr BP) from Murray Springs and AA-25778 (10,260 ± 85 ^{14}C yr BP) from Big Eddy for YDB_{Obs}, as well as Kruft samples HD-19092 (11,066 ± 28 ^{14}C yr BP), HD-18622 (11,073 ± 33 ^{14}C yr BP), and HD-19037 (11,075 ± 28 ^{14}C yr BP) for LST. TX-1044 is a non-AMS measurement on charcoal, and we have scored this measurement as a potential "old wood" sample. It was excluded in the main YDB_{Obs} dataset due to its anomalously large error, which is at least an order of magnitude larger than any other error in YDB_{Obs}, and importantly, much larger than the errors reported in the VIRI dataset to which the LBM was fitted. As such, it is unknown whether the LBM provides realistic parameter values for how much intra- and interlaboratory measurement variability should be expected with an error this large. We excluded AA-25778 from the main YDB_{Obs} dataset since this measurement came from a wood charcoal specimen with potential redeposition issues, so its spatial association with the YDB layer is not secure (Wittke et al., 2013). We have scored this as another potential "old wood" sample. The three Kruft samples all correspond to LST_{Obs} measurements from a series of adjacent tree rings from the same wood specimen, designated as *Populus* 9 (Baales et al., 1998, 2002). We included the most recent *Populus* 9 date in the main LST_{Obs} dataset, HD-19098 (11,063 ± 30 ^{14}C yr BP). The three excluded *Populus* 9 measurements must logically date to earlier than HD-19098 and have a known chronological order that predates the LST, the sequence of which is not captured in the simulation. For Alternative 1, we have included these measurements and scored all three as potential "old wood" samples. Alternative 1 is the most inclusive set of measurements that we could construct for LST_{Obs} and YDB_{Obs}. Notably, Alternative 1 LST_{Obs} is more tightly clustered than the main LST_{Obs} dataset (Table 5). In contrast, for YDB_{Obs}, the values for Alternative 1 suggest a more dispersed set of measurements than those in the main dataset.

Table 4. Comparison of LST_{Obs} and YDB_{Obs}.

	LST_{Obs} (n = 19)	YDB_{Obs} (n = 30)
n sites	6	13
n accelerator mass spectrometry measurements	0 (0.0%)	27 (90.0%)
n unique laboratories	6	8
n "old wood" measurements	18 (94.7%)	24 (80.0%)
Average ^{14}C measurement error	94.47	59.00
$\sigma^{14}C$	196.94	282.02
Dissimilarity	0.71	0.75

Alternative 2 excludes three YDB_{Obs} ^{14}C measurements that were included in the main YDB_{Obs} dataset: Beta-184854 (11,070 ± 60 ^{14}C yr BP) from Bull Creek, TX-1045 (10,260 ± 140 ^{14}C yr BP) from Murray Springs, and AA-27864 (11,900 ± 80 ^{14}C yr BP) from Big Eddy. These values were excluded due to the possibility that dispersion in YDB_{Obs} may be driven by unreliable measurements. As such, removing these measurements could lead to a YDB_{Obs} that is more consistent YDB_{Sim}. In effect, Alternative 2 is an attempt to bias YDB_{Obs} in a manner favorable to the synchroneity requirement of the Younger Dryas Impact Hypothesis, based on reasonable arguments that a researcher might make about excluding observations in YDB_{Obs}.

https://doi.org/10.1017/qua.2019.83 Published online by Cambridge University Press

Table 5. Sample sizes and average lab errors for the three alternative observed datasets.

	n ^{14}C measurements (average lab error)		Dissimilarity		σ^{14}C	
Dataset	LST	YDB	LST	YDB	LST	YDB
Main dataset	19 (94.47)	30 (59.00)	0.71	0.75	196.94	282.02
Alternative 1	22 (85.64)	32 (134.22)	0.68	0.78	182.56	416.64
Alternative 2	19 (94.47)	27 (55.19)	0.71	0.72	196.94	190.65
Alternative 3	9 (115.44)	18 (74.17)	0.60	0.70	156.94	315.32

Beta-184854 and TX-1045 are from SOM, which represent values for the time-averaged death and deposition dates of many small organisms within each sample's respective stratum. Dates corresponding to SOM measurements do not represent to a single event, and they generally postdate the depositional event of interest due to continued input of organic matter into a geological layer (Wang et al., 1996). This potential issue is supported by the observation that TX-1045 is 350 ^{14}C yr younger than the next youngest measurement in YDB_{Obs}, UCIAMS-29317 (10,610 ± 25 ^{14}C yr BP). Unlike TX-1045, Beta-184854 is not anomalously young, but we have excluded it since the measurement is also from a SOM sample.

AA-27864 is not a SOM measurement, but rather a measurement on charcoal. We have excluded it because it is anomalously old, at 460 ^{14}C yr older than the next oldest measurement in YDB_{Obs}, UCIAMS-36961. Although we do not feel that it is justified to remove AA-27486 based on its age alone—hence, why we included it in our main YDB_{Obs} dataset—we anticipate that other researchers might consider its exclusion. In combination, removing these three measurements produces an Alternative 2 YDB_{Obs} that appears more consistent with synchroneity than does the main YDB_{Obs} dataset (Table 5).

Alternative 3 eliminates the Arlington Canyon measurements ($n = 12$) from YDB_{Obs} and the Brohl Valley measurements ($n = 10$) from LST_{Obs}. Samples from these two sites represent 40.0 and 52.6% of each respective observed dataset, contributing a disproportionately large share of measurements. As such, any site-level factors that affect the dispersion of ^{14}C measurements within each site could have an outsized effect on either YDB_{Obs} or LST_{Obs}. When measurements from these two sites are removed, σ^{14}C and dissimilarity values are reduced and remain consistent with synchroneity for the LST_{Obs} (Table 5). For the YDB_{Obs}, the dissimilarity value appears more consistent with synchroneity, but the σ^{14}C value becomes more dispersed and inconsistent with synchroneity.

We also repeat the simulations for the main dataset and each alternative dataset with all observed measurements scored as AMS. Due to the role of the AMS vs GPC/LSC distinction in the LBM, the disparity in the number of AMS measurements between LST_{Obs} and YDB_{Obs} (Table 4) has the potential to create very different expectations regarding the distribution of simulated datasets for each event. Although we argue that it is best to account for these methodological differences when generating expectations for each event, we also explore the consequences of ignoring this aspect of ^{14}C measurement.

RESULTS

For each of six simulations we present results comparing the observed datasets (LST_{Obs} and YDB_{Obs}) to the simulated datasets (LST_{Sim} and YDB_{Sim}). The six simulations represent three old wood models (OWM)—no OWM, a smaller offset OWM, and a larger OWM—with the inclusion or exclusion of measurement offsets randomly sampled from the LBM (Table 3). Figure 4 is an annotated diagram of the results of a mock simulation that aids in interpreting the graphical results displayed in Figures 5–10.

Simulation A1

Simulation A1 does not account for any sources of uncertainty in the dataset, except for those inherent in the process of measuring and calibrating ^{14}C dates. LST_{Sim} and YDB_{Sim} are much more clustered than the observed datasets, both in terms of σ^{14}C and dissimilarity values (Fig. 5a and b). The median σ^{14}C values range from 5.69 to 5.85 across the 101 simulated yr, far smaller, and thus more clustered, than the LST_{Obs} and YDB_{Obs} σ^{14}C values (196.94 and 282.02, respectively). Similarly, the median simulated dissimilarity values range between 0.16 and 0.27, indicating that after recalibration, the simulated datasets are still much more clustered than LST_{Obs} and YDB_{Obs} (dissimilarity values of 0.71 and 0.75, respectively).

No iteration of simulation A1 (10,000 iterations per each of 101 yr for each of two events, or 2.02e6 total iterations) produced a ^{14}C dataset that was as or more dispersed than either LST_{Obs} or YDB_{Obs}. As such, we are unable to use simulation samples to directly estimate the probability of simulation A1 generating synchronous datasets as dispersed as the observed datasets. To calculate this probability, we first log-transformed the simulated σ^{14}C values (LST_{Sim} and YDB_{Sim}) and the σ^{14}C value of the observed datasets (LST_{Obs} or YDB_{Obs}) to approximate normal distributions. We then calculated the z-score for the log-transformed observed value within each year's log distribution of simulated values. Similarly, we logit transformed the dissimilarity values to approximate normality, and

https://doi.org/10.1017/qua.2019.83 Published online by Cambridge University Press

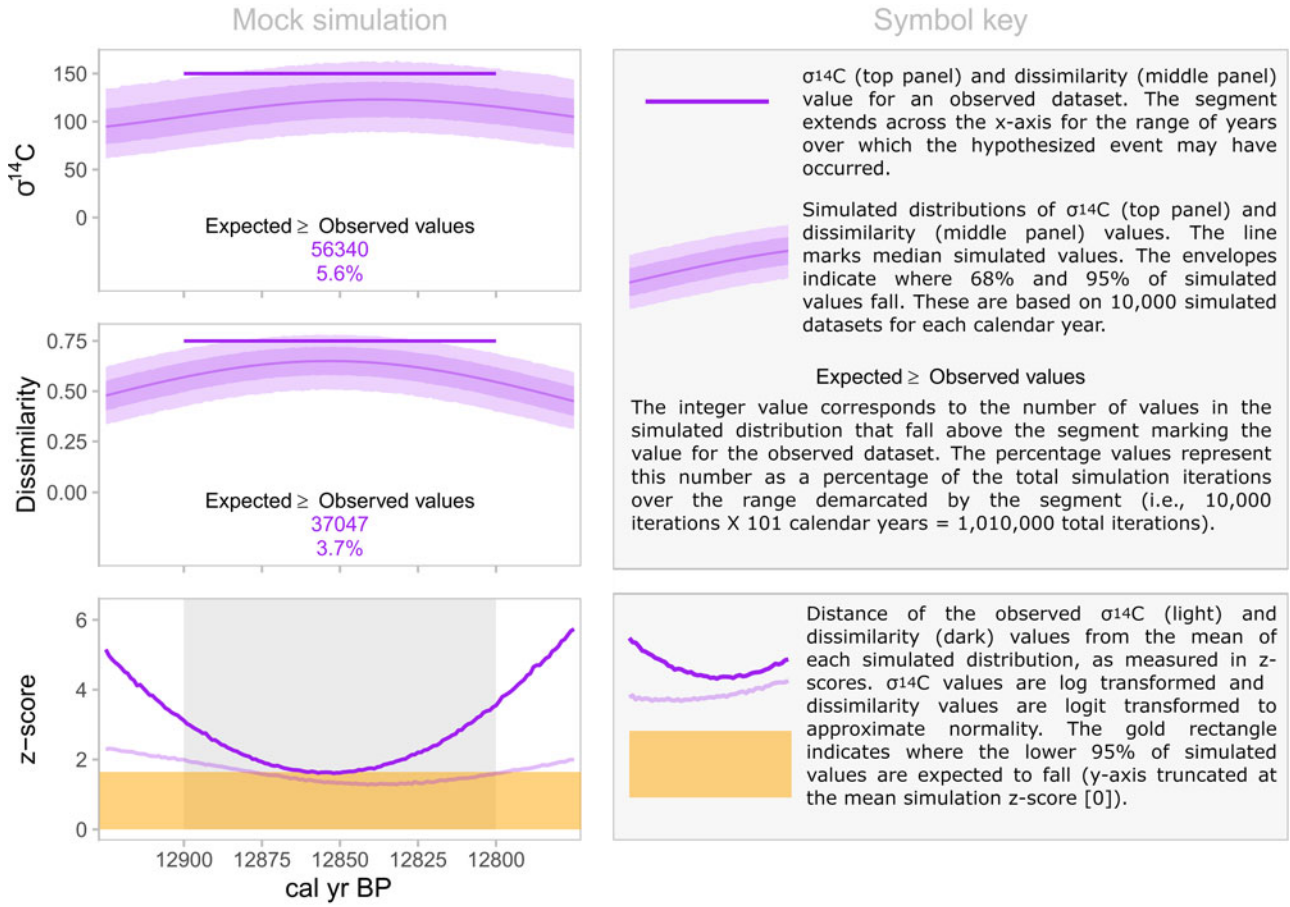

Figure 4. (color online) A mock simulation demonstrating the graphical presentation of simulation results for both clustering measures: $\sigma^{14}C$ and dissimilarity. Here, a synchronous event is hypothesized to have occurred between 12,900 and 12,800 cal BP, as indicated by the segment in the top two panels. Results show that the clustering values in the observed dataset (0.75 and 150) are improbable given a synchronous event in any year within this range. However, this low probability is not constant, as the calibration curve affects the degree of expected clustering. Synchronous events within ~12,870–12,830 cal BP are relatively more likely to produce datasets like the observed dataset than are other years in the hypothesized range, although this probability remains low.

calculated the z-scores for the logit observed values within the logit simulated dissimilarity value distributions for each year. Both observed datasets are extremely improbable if the underlying events that produced them were synchronous (Fig. 5c). At best, the observed datasets are more than nine z-scores more dispersed than the simulated datasets, and at worst nearly 80 z-scores more dispersed. The probability of obtaining a z-score of nine is astronomically small. These results are unsurprising, as simulation A1 does not account for any sources of uncertainty in the dataset, except for those inherent in the process of measuring and calibrating ^{14}C dates. Since we assume that the LST was produced by a synchronous event, we conclude that simulation A1 does not fully capture the sources of uncertainty in the observed datasets.

Simulation A2

Simulation A2 differs from A1 in that it applies offsets drawn randomly from the LBM to the target ^{14}C values to produce measured ^{14}C values that incorporate variability driven by the number and types of labs in LST_{Obs} and YDB_{Obs} (Table 3). The additional variability introduced by the inclusion of the LBM offsets produced LST_{Sim} ^{14}C datasets that are somewhat more dispersed than in A1. However, the median simulated $\sigma^{14}C$ (47.69–48.63) and dissimilarity values (0.36–0.37) are still well below the observed values. Similarly, simulation A2 produced YDB_{Sim} datasets that are more dispersed than in A1, but still much more clustered than YDB_{Obs}. The median simulated $\sigma^{14}C$ values range between 26.25 and 26.58, and the median simulated dissimilarity values range from 0.23 to 0.33 (Fig. 6a and b).

While both LST_{Sim} and YDB_{Sim} generated median values indicating much more clustering than in their respective observed datasets, some LST_{Sim} iterations generated datasets as or more dispersed than LST_{Obs} (Fig. 6a and b). However, this was not the case for any iterations of YDB_{Sim}. This is reflected in the z-scores; the LST_{Obs} $\sigma^{14}C$ value is 1.8 z-scores above the mean $\sigma^{14}C$ simulated value for a given year, and the observed dissimilarity value is 2.3 z-scores above the mean simulated value (Fig. 6c). The YDB_{Obs} z-scores range between 5.5 and 6.9, indicating a dataset that is still extremely improbable given the results of the

https://doi.org/10.1017/qua.2019.83 Published online by Cambridge University Press

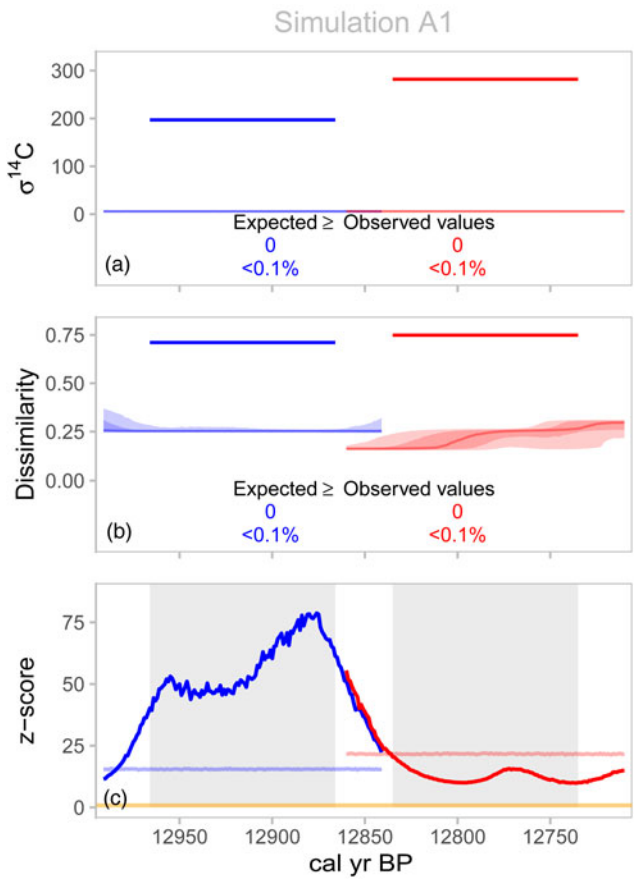

Figure 5. Results for simulation A1, which did not incorporate an LBM or OWM: (a) $\sigma^{14}C$ results, (b) dissimilarity results, and (c) distance between the observed and the mean simulated $\sigma^{14}C$ and dissimilarity values. Blue geometry corresponds to LST results (left side), and red geometry corresponds to YDB results (right side). Refer to Figure 4 for symbol key. (For interpretation of the references to color in this figure legend, the reader is referred to the web version of this article.)

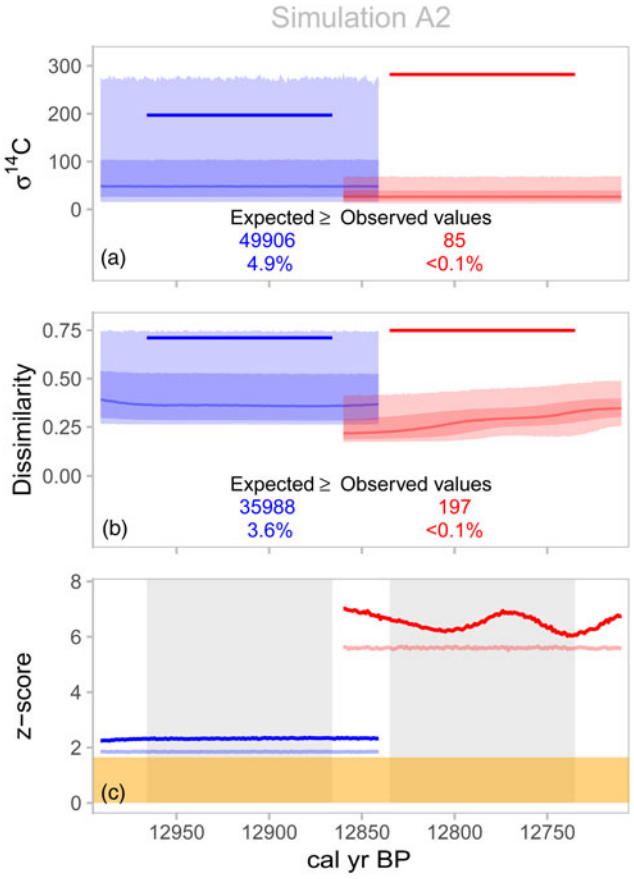

Figure 6. Results for simulation A2, which incorporated the LBM but not an OWM: (a) $\sigma^{14}C$ results, (b) dissimilarity results, and (c) distance between the observed and the mean simulated $\sigma^{14}C$ and dissimilarity values. Blue geometry corresponds to LST results (left side), and red geometry corresponds to YDB results (right side). Refer to Figure 4 for symbol key.

simulation (at z-score = 5.5, $p \approx$ 1.9e-8). Inclusion of the LBM begins to capture more of the variability found in the LST_{Obs} dataset, but with median simulated $\sigma^{14}C$ and dissimilarity values well below the observed values, simulation A2 does not fully capture the sources of uncertainty in the observed datasets.

Simulation B1

Simulation B1 includes conservative OWM age offsets, but not offsets from the LBM. Inclusion of the conservative OWM offsets in simulation B1 increases the dispersion of LST_{Sim} and YDB_{Sim} datasets, compared to simulation A1, but does not result in any iterations with $\sigma^{14}C$ or dissimilarity values as large as LST_{Obs} or YDB_{Obs} (Fig. 7a and b). Thus, this simulation also fails to capture the variability of the observed datasets. Both LST_{Obs} and YDB_{Obs} remain extremely improbable, with LST_{Obs} z-scores ranging from 6.1 to 10.9 as measured with $\sigma^{14}C$ and ranging from 9.4 to 27.8 as measured with dissimilarity. YDB_{Obs} z-scores range from 7.9 to 13.2 and from 6.9 to 15.2, for $\sigma^{14}C$ and dissimilarity respectively (Fig. 7c). There is greater variability in the range of simulated values across years, and thus z-score values across years, than in simulations A1 or A2. Since the OWM age offsets are applied to target ^{14}C values before recalibration, they shift the target ^{14}C values earlier in the calibration curve, in some cases into regions of the curve with a different slope. This can lead, in some calendar years, to increased clustering of dates when shifted into steeper regions of the curve, or increased dispersion when shifted into flatter regions of the curve.

Simulation B2

This simulation combines conservative OWM offsets, as in simulation B1, with offsets drawn from the LBM, as in simulation A2. Simulation B2 produced $\sigma^{14}C$ and dissimilarity values generally similar in magnitude to the values generated by simulation A2, but with increased variability across calendar years as in simulation B1, indicating that the two different offset models impact the results of the simulation in different ways. As in previous simulations, there is a clear difference between LST_{Sim} and YDB_{Sim}. A total of 5.1% of LST_{Sim}

https://doi.org/10.1017/qua.2019.83 Published online by Cambridge University Press

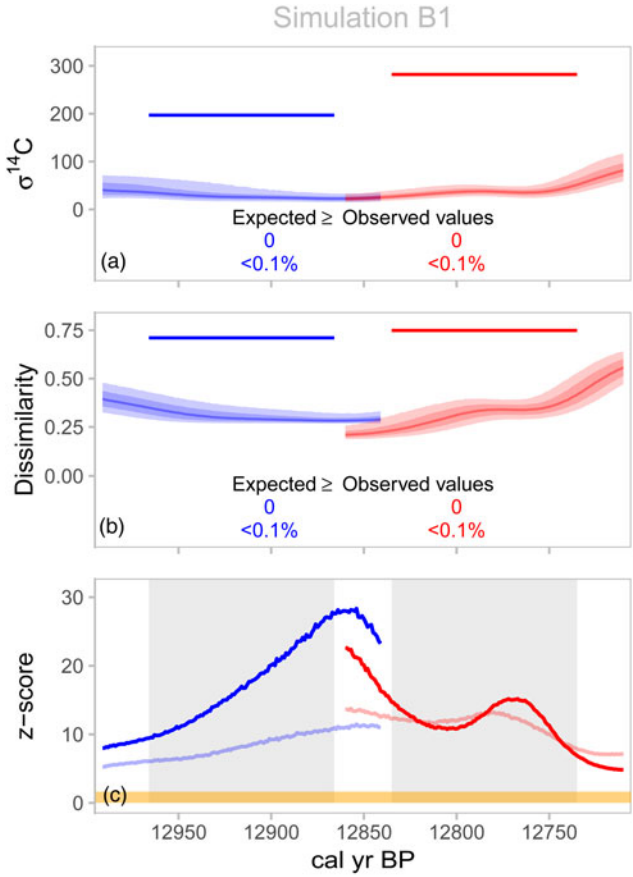

Figure 7. Results for simulation B1, which did not incorporate an LBM but did use the OWM that assumed minor old woods effects ($\lambda = 0.04$): (a) $\sigma^{14}C$ results, (b) dissimilarity results, and (c) distance between the observed and the mean simulated $\sigma^{14}C$ and dissimilarity values. Blue geometry corresponds to LST results (left side), and red geometry corresponds to YDB results (right side). Refer to Figure 4 for symbol key. (For interpretation of the references to color in this figure legend, the reader is referred to the web version of this article.)

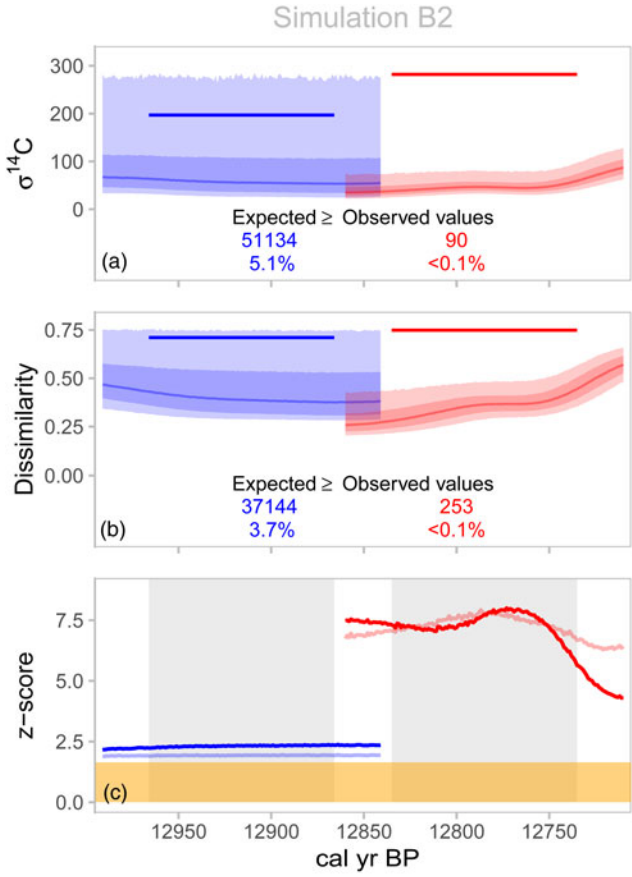

Figure 8. Simulation B2, which incorporated the LBM and the OWM that assumed minor old wood effects ($\lambda = 0.04$): (a) $\sigma^{14}C$ results, (b) dissimilarity results, and (c) distance between the observed and the mean simulated $\sigma^{14}C$ and dissimilarity values. Blue geometry corresponds to LST results (left side), and red geometry corresponds to YDB results (right side). Refer to Figure 4 for symbol key. (For interpretation of the references to color in this figure legend, the reader is referred to the web version of this article.)

iterations produced $\sigma^{14}C$ values as larger or larger than LST_{Obs}, while 3.7% of iterations generated dissimilarity values. Fewer than 0.1% of YDB_{Sim} iterations produced $\sigma^{14}C$ or dissimilarity values exceeding the YDB_{Obs} values. The LST_{Obs} $\sigma^{14}C$ value is 1.9 or more z-scores above the mean simulated $\sigma^{14}C$ value for a given year in simulation B2, and the observed dissimilarity value is 2.3 or more z-scores above the mean simulated value. The YDB_{Obs} z-scores range between 5.6 and 8.0 above the mean YDB_{Sim} $\sigma^{14}C$ and dissimilarity values, indicating a dataset that is improbably dispersed given the results of the simulation.

Simulation C1

This simulation incorporates a more extreme OWM offset, but no offsets drawn from the LBM. As expected, the larger OWM offset drives additional dispersion of the simulated datasets (Fig. 9a and b) compared to simulation B1. A total of 1.7% of LST_{Sim} iterations have a $\sigma^{14}C$ value as large as or larger than LST_{Obs}, while <0.1% of YDB_{Sim} iterations have a $\sigma^{14}C$ value as large as or larger than YDB_{Obs}. Only a few iterations of LST_{Sim} have dissimilarity values as large as or larger than LST_{Obs}, and no YDB_{Sim} iterations approach the dissimilarity value of YDB_{Obs}. The z-scores for LST_{Obs} indicate that this dataset is still relatively improbable given the distribution of the simulation; YDB_{Obs} z-scores are much larger than LST_{Obs} z-scores, and thus YDB_{Obs} remains extremely improbable (Fig. 9c).

The median $\sigma^{14}C$ and dissimilarity values generated by simulation C1 are closer to LST_{Obs} and YDB_{Obs} than in any previous simulation. However, simulations A2 and B2 capture more iterations with datasets as or more dispersed than the observed datasets. This indicates that while the extreme OWM drives greater average dispersion, the LBM leads to the more frequent appearance of very dispersed iterations.

Simulation C2

Simulation C2 includes the offsets drawn from the more extreme OWM and offsets from the LBM. This simulation

https://doi.org/10.1017/qua.2019.83 Published online by Cambridge University Press

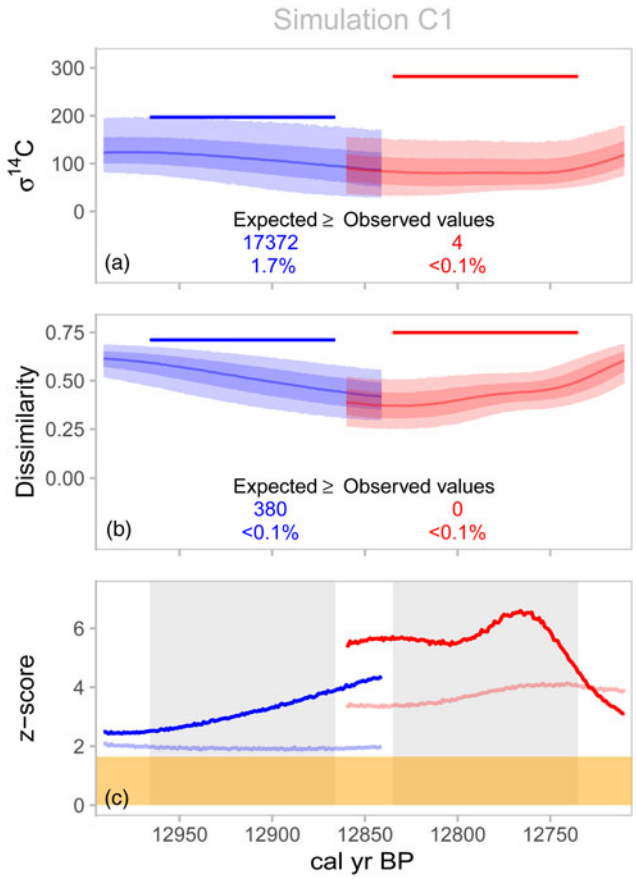

Figure 9. Results for simulation C1, which did not incorporate an LBM but did use the OWM that assumed minor old woods effects ($\lambda = 0.01$): (a) $\sigma^{14}C$ results, (b) dissimilarity results, and (c) distance between the observed and the mean simulated $\sigma^{14}C$ and dissimilarity values. Blue geometry corresponds to LST results (left side), and red geometry corresponds to YDB results (right side). Refer to Figure 4 for symbol key. (For interpretation of the references to color in this figure legend, the reader is referred to the web version of this article.)

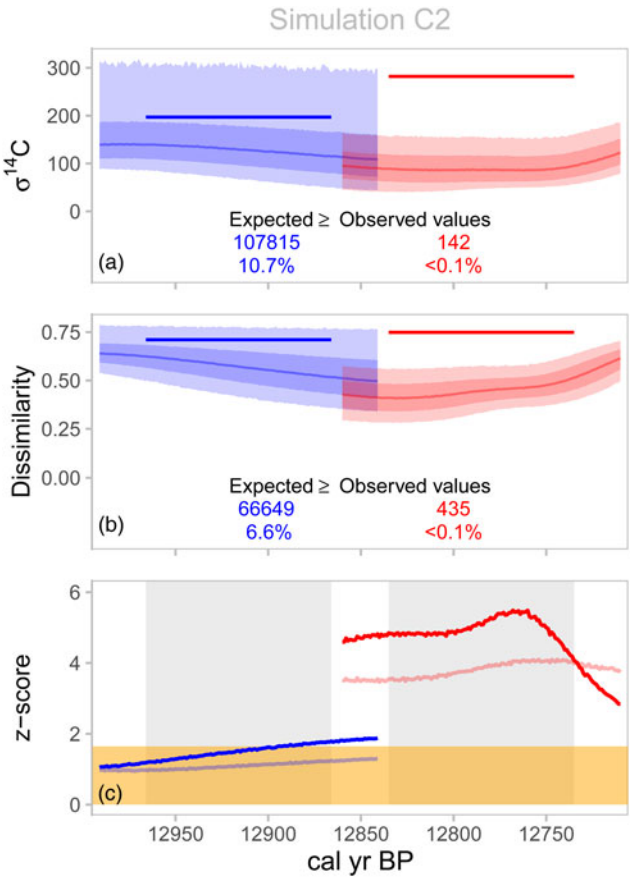

Figure 10. Results for simulation C2, which incorporated the LBM and the OWM that assumed minor old woods effects ($\lambda = 0.01$): (a) $\sigma^{14}C$ results, (b) dissimilarity results, and (c) distance between the observed and the mean simulated $\sigma^{14}C$ and dissimilarity values. Blue geometry corresponds to LST results (left side), and red geometry corresponds to YDB results (right side). Refer to Figure 4 for symbol key. (For interpretation of the references to color in this figure legend, the reader is referred to the web version of this article.)

includes the most sources of variability in the underlying processes driving dispersion in ^{14}C measurements, and it is therefore likely the simulation that most closely approximates the processes that acted on the observed ^{14}C datasets. The combination of both sources of variability produced LST_{Sim} distributions with median $\sigma^{14}C$ and dissimilarity values that are larger than in the previous five simulations, indicating more dispersed datasets (Fig. 10a and b). For LST_{Sim}, median $\sigma^{14}C$ values range from 115.58 to 139.95 and median dissimilarity values range from 0.52 to 0.62. A total of 10.7 and 6.6% of LST_{Sim} iterations produced $\sigma^{14}C$ or dissimilarity values as larger or larger than LST_{Obs}, respectively. These results indicate that the amount of dispersion observed in the LST dataset is not improbable for a synchronous event, once potential sources of ^{14}C variability are accounted for in the simulation.

In contrast, while simulation C2 produced YDB_{Sim} distributions indicating more dispersion than in previous simulations, simulated $\sigma^{14}C$ and dissimilarity values do not approach the observed YDB values. While some iterations produced $\sigma^{14}C$ (<0.1%) or dissimilarity (<0.1%) values as large or larger than YDB_{Obs}, median YDB_{Sim} values are much more clustered than YDB_{Obs}. This is reflected in the z-scores for YDB_{Obs}, which range from 3.5 to 5.5 (Fig. 10c). The probability of obtaining an iteration 3.5 z-scores larger than the mean value is 2.3e-4, roughly four orders of magnitude less likely than the probability, given LST_{Sim}, of generating values as large or larger than LST_{Obs}.

The results of simulation C2 illustrate that even when many sources of variability are incorporated, it is improbable that a synchronous event could produce a ^{14}C dataset as dispersed as YDB_{Obs}.

Alternative observed datasets

Due to the amount of simulation output across these alternative datasets (42 simulations), we provide only a brief overview of results of the alternative observed datasets here, focusing on C2 simulations. The full quantitative and

https://doi.org/10.1017/qua.2019.83 Published online by Cambridge University Press

Table 6. Results from alternative dataset simulations. Numbers represent the number of values in simulation C2 that were greater than or equal to observed values. Parenthetical values are the percentage of simulated values that were greater than observed values (out of 1,010,000).

	$\sigma^{14}C$		Dissimilarity	
	LST	YDB	LST	YDB
Main dataset	107,815 (10.7%)	142 (<0.1%)	66,649 (6.6%)	435 (<0.1%)
Main dataset (all as AMS)	44,292 (4.4%)	202 (<0.1%)	17,252 (1.7%)	291 (<0.1%)
Alternative 1	142,906 (14.2%)	35 (<0.1%)	156,349 (15.5%)	301 (<0.1%)
Alternative 1 (all as AMS)	63,083 (6.3%)	14 (<0.1%)	55,929 (5.5%)	237 (<0.1%)
Alternative 2	109,051 (10.8%)	4907 (0.5%)	67,970 (6.7%)	913 (0.1%)
Alternative 2 (all as AMS)	44,349 (4.4%)	4509 (0.5%)	17,782 (1.8%)	775 (0.1%)
Alternative 3	285,931 (28.3%)	147 (<0.1%)	440,622 (43.6%)	638 (0.1%)
Alternative 3 (all as AMS)	195,964 (19.4%)	65 (<0.1%)	327,356 (32.4%)	442 (<0.1%)

graphical results of the alternative dataset simulations are presented as Supplementary Data.

Alternative 1 simulations, which included the five ^{14}C measurements that were excluded from YDB_{Obs} and LST_{Obs}, were broadly comparable to those for the main observed datasets. Alternative 1 LST_{Obs} became modestly more probable, with the percentage of simulated $\sigma^{14}C$ values exceeding the observed value increasing from 10.7 to 14.2% and from 6.6 to 15.5% for dissimilarity values (Table 6). However, results simulated using Alternative 1 YDB_{Obs} remained relatively unchanged from the original YDB_{Obs} dataset, with the percentages of simulated values that exceeded observed values remaining well below 0.1% for both measures.

For Alternative 2 simulations, which exclude three YDB_{Obs} ^{14}C measurements that were included in the main YDB_{Obs} dataset, YDB_{Obs} was modestly more probable regarding dissimilarity value outcomes, increasing from <0.1 to 0.1% of iterations that exceed the observed value. Alternative 2 YDB_{Obs} was over an order of magnitude more probable for $\sigma^{14}C$ outcomes relative to the main YDB_{Obs} dataset, increasing from <0.1 to 0.5%. However, even with these increases, the probability of observing the amount of dispersion displayed in Alternative 2 YDB_{Obs} remains below 1% and well below the probabilities for LST_{Obs}. Alternative 2 LST_{Obs} is the same dataset as the main LST_{Obs} dataset. Slight differences in the main dataset and Alternative 2 dataset outcome for LST_{Obs}, as displayed in Table 6, are due entirely to simulation variance.

For Alternative 3, which eliminates the Arlington Canyon measurements ($n = 12$) from YDB_{Obs} and the Brohl Valley measurements ($n = 10$) from LST_{Obs}, LST_{Obs} becomes much more probable relative to the main dataset, with an increase of 10.7 to 28.3% for simulated $\sigma^{14}C$ values that exceed the observed value and an increase of 6.6 to 43.6% for dissimilarity values. Simulations using Alternative 3 YDB_{Obs} remain mostly unchanged from the main YDB_{Obs} dataset, with less than 0.1% of simulated values exceeding observed values for both measures.

In all alternative dataset simulations that incorporate the LBM, scoring all observed measurements as AMS increased clustering in the simulated datasets. As such, both LST_{Obs} and YDB_{Obs} became less probable, although this effect was much larger for LST_{Obs} (Table 6). This difference was expected since the LST_{Obs} datasets lack AMS measurements entirely. Even with these differences, simulated outcomes for the LST_{Obs} dataset remain at least an order of magnitude more probable than the simulated outcomes for YDB_{Obs}. As such, differences in the simulated results for each event probably cannot be attributed to how the LBM handles dispersion in AMS vs GPC/LSC measurements.

DISCUSSION

For the Laacher See volcanic eruption, the known synchronous event, our simulations generated $\sigma^{14}C$ and dissimilarity values comparable to the LST_{Obs} $\sigma^{14}C$ and dissimilarity values, but only when we incorporated the LBM and the OWM with the larger offsets as simulation parameters. This suggests that if known sources of uncertainty are incorporated into the simulations, the simulations generate realistic expectations for clustering in a set of ^{14}C measurements. While simulation C2 produced many LST_{Sim} iterations with $\sigma^{14}C$ and dissimilarity values greater than the LST_{Obs} values, mean simulated $\sigma^{14}C$ and dissimilarity values are smaller than their observed counterparts across all calendar years, likely due to additional sources of variability left unaddressed by our simulations. It is possible that our LBM, based on recent data from the Fifth International Radiocarbon Intercomparison (Scott et al., 2007, 2010a, 2010b), does not fully capture the inter- and intralaboratory variability that existed in the 1950s and 1960s, when several of the LST ^{14}C values were first measured. This would not be the case with the YDB_{Obs} values, as only one was originally measured in the 1950s, two measured in 1975 and 1981, and the remaining YDB_{Obs} values in the 1990s or later. Similar issues might arise in other observed legacy datasets for known synchronous events dominated by older values, such as the Mt. Mazama eruption in North America (Egan et al., 2015). Additional known synchronous events with recent ^{14}C values could provide further evaluation of our method (e.g., Friedrich et al., 2006; Christen and Pérez, 2009; Okuno et al., 2010).

https://doi.org/10.1017/qua.2019.83 Published online by Cambridge University Press

In contrast to the LST simulations, the YDB simulations produced $\sigma^{14}C$ and dissimilarity values that are far more clustered than those for YDB_{Obs}. Even when incorporating the LBM and the OWM that allows for the larger age offsets, simulation C2 produced YDB_{Sim} datasets that rarely reach the amount of dispersion present in YDB_{Obs}, with observed values at 3.5 or more z-scores above the mean simulated values ($p \leq 2.3e\text{-}4$). The disparity between YDB and LST results is not a function of the difference in the sample sizes of LST_{Obs} and YDB_{Obs} (Supplementary Data).

While one might expect that synchronous events would produce roughly equally clustered observed datasets for each event, these two observed datasets are differentiated by three features that explain the divergent simulation outcomes: (1) LST_{Obs} has proportionally more wood-based ^{14}C measurements (18/19) than YDB_{Obs} (24/30), (2) LST_{Obs} has a larger average ^{14}C measurement error than YDB_{Obs}, and (3) none of the LST_{Obs} measurements are AMS, while 27 of 30 YDB_{Obs} measurements are AMS. AMS measurements are generally more precise than alternative methods, as is borne out by the LBM (Supplementary Data). These differences in sources of variability between YDB_{Obs} and LST_{Obs} indicate that if YDB_{Obs} corresponds to a synchronous event, it should be *more* clustered than LST_{Obs}. Yet, YDB_{Obs} is *less* clustered than LST_{Obs}.

Why do our results differ from those of Kennett et al. (2015), who concluded that the YDB was deposited synchronously across multiple continents? Kennett et al. base their conclusion on modelled YDB age densities from 23 sites with purported extraterrestrial impact markers, estimated dates of six climatic proxies for the onset of the Younger Dryas, and the date of a platinum peak that appears in the GISP2 Greenland ice core. They assigned these thirty age distributions to a single phase, representing the depositional duration of the YDB, and modeled the posterior age distributions for the temporal boundaries of the phase. Finally, they calculated the distribution of possible age differences between those boundaries. Since the 95.4% interval of possible differences (-5 and 130 years) between the start and end of their phase includes zero (Kennett et al. 2015, Table S28), they conclude that synchroneity is possible.

We agree that synchroneity is *possible*, but our simulations demonstrate that it is extremely *improbable* that a synchronous event could produce ^{14}C measurements as dispersed as those in YDB_{Obs}. The most parsimonious explanation for the large difference in clustering between YDB_{Sim} and YDB_{Obs} is that the observed measurements were deposited asynchronously over multiple years, rather than by a single event. The Younger Dryas Impact Hypothesis "requires dates on the YDB layer to be essentially isochronous across four continents within the limits of dating methods" (Kennett et al., 2015, p. 4344). The results of our simulations establish that this requirement is not met.

CONCLUSION

Radiocarbon dating is vital to late Quaternary research. However, transforming a ^{14}C measurement into a calendar age is complex, and results are typically not precise enough to evaluate hypotheses requiring decadal or annual scale precision. To overcome this limitation, we introduced a Monte Carlo simulation-based approach to evaluate whether a set of ^{14}C measurements is consistent with the hypothesis that the ^{14}C samples measured were deposited synchronously. We first evaluated this method using the ^{14}C measurements associated with the Laacher See volcanic eruption. Simulated sets of synchronous ^{14}C measurements are consistent with the observed Laacher See ^{14}C measurements, and thus consistent with a conclusion that the Laacher See ^{14}C samples were deposited synchronously. We then applied this method to a set of ^{14}C measurements associated by Kennett et al. (2015) with the Younger Dryas Extraterrestrial Impact Hypothesis. Simulation results demonstrate that these ^{14}C samples were extremely unlikely to have been deposited synchronously, calling into question a key logical requirement of this hypothesis. In sum, our results fail to support the claim that there was an extraterrestrial impact ~12,800 cal yr BP that was responsible for Younger Dryas climatic cooling, Terminal Pleistocene megafaunal extinctions, widespread burning, and the disappearance of the Clovis archaeological culture.

ACKNOWLEDGMENTS

Simulations were completed on the ManeFrame II cluster at Southern Methodist University, with assistance from Robert Kalescky. Comments from Jeff Pigati, Nicholas Lancaster, and two anonymous reviewers improved our paper. David Meltzer read multiple early drafts of the manuscript and provided invaluable feedback. Enrico Crema kindly responded to our queries regarding the *rcarbon* R package and provided advice on this manuscript. Maarten Blaauw and Matthew Boulanger also gave helpful comments. This work was completed without funding.

SUPPLEMENTARY MATERIAL

The supplementary material for this article can be found at https://doi.org/10.1017/qua.2019.83.

REFERENCES CITED

Aura Tortosa, J.E., Miret i Estruch, C., Morales Pérez, J.V., 2008. Coves de Santa Maira (Castell de Castells, La Marina Alta, Alacant). Campaña de 2008. *Saguntum* (*P.L.A.V.*) 40, 227–232.

Baales, M., Bittmann, F., Kromer, B., 1998. Verkohlte Bäume im Trass der Laacher See-Tephra bei Kruft (Neuwieder Becken): Ein Beitrag zur Datierung des Laacher See-Ereignisses und zur Vegetation der Allerød-Zeit am Mittelrhein. *Archäeologisches Korrespoindenzblatt* 28, 191–204.

Baales, M., Jöris, O., Street, M., Bittmann, F., Weninger, B., Wiethold, J., 2002. Impact of the Late Glacial eruption of the Laacher See Volcano, Central Rhineland, Germany. *Quaternary Research* 58, 273–288.

Baillie, M.G.L., 1991. Suck in and smear: Two related chronological problems for the 90s. *Journal of Theoretical Archaeology* 2, 12–16.

Bement, L.C., Madden, A.S., Carter, B.J., Simms, A.R., Swindle, A.L., Alexander, H.M., Fine, S., Benamara, M., 2014.

Quantifying the distribution of nanodiamonds in pre-Younger Dryas to recent age deposits along Bull Creek, Oklahoma Panhandle, USA. *Proceedings of the National Academy of Sciences of the United States of America* 111, 1726–1731.

Bengtsson, H., Bravo, H.C., Gentleman, R., Hossjer, O., Jaffee, H., Jian, D., Langfelder, P., Hickey, P., 2018. matrixStats: Functions that apply to rows and columns of matrices (and to vectors). https://cran.rstudio.com/web/packages/matrixStats/index.html, accessed June 15, 2019.

Bergin, K.A., 2011. The archaeology of the Talega Site (CA-ORA-907), Orange County, California: Perspective on the prehistory of southern California. Prepared for the District of the US Army Corps of Engineers, Los Angeles.Viejo California Associates, Mission Viejo.

Bevan, A., Crema, E., 2018. rcarbon v1.1.3: Methods for calibrating and analyzing radiocarbon dates. https://cran.r-project.org/web/packages/rcarbon/index.html, accessed June 15, 2019.

Blaauw, M., Holliday, V.T., Gill, J.L., Nicoll, K., 2012. Age models and the Younger Dryas Impact Hypothesis. *Proceedings of the National Academy of Sciences of the United States of America* 109, E2240. https://doi.org/10.1073/pnas.1206143109

Boaretto, E., Bryant, C., Carmi, I., Cook, G., Gulliksen, S., Harkness, D., Heinemeier, J., McClure, J., McGee, E., Naysmith, P., 2003. How reliable are radiocarbon laboratories? A report on the Fourth International Radiocarbon Inter-comparison (FIRI) (1998–2001). *Antiquity* 77, 146–154.

Boslough, M., Nicoll, K., Holliday, V.T., Daulton, T.L., Meltzer, D., Pinter, N., Scott, A.C., *et al.*, 2012. Arguments and evidence against a Younger Dryas impact event. *Geophysical Monograph Series* 198, 13–26.

Bronk Ramsey, C., 2008. Radiocarbon dating: Revolutions in understanding. *Archaeometry* 50, 249–275.

Bronk Ramsey, C., 2009a. Bayesian analysis of radiocarbon dates. *Radiocarbon* 51, 337–360.

Bronk Ramsey, C., 2009b. Dealing with outliers and offsets in radiocarbon dating. *Radiocarbon* 51, 1023–1045.

Bunch, T.E., Hermes, R.E., Moore, A.M.T., Kennett, D.J., Weaver, J.C., Wittke, J.H., DeCarli, P.S., *et al.*, 2012. Very high-temperature impact melt products as evidence for cosmic airbursts and impacts 12,900 years ago. *Proceedings of the National Academy of Sciences of the United States of America* 109, E1903–E1912.

Christen, J.A., Pérez, E.S., 2009. A new robust statistical model for radiocarbon data. *Radiocarbon* 51, 1047–1059.

Daulton, T.L., Amari, S., Scott, A.C., Hardiman, M., Pinter, N., Anderson, R.S., 2017. Comprehensive analysis of nanodiamond evidence relating to the Younger Dryas Impact Hypothesis: The nanodiamond evidence. *Journal of Quaternary Science* 32, 7–34.

Daulton, T.L., Pinter, N., Scott, A.C., 2010. No evidence of nanodiamonds in Younger-Dryas sediments to support an impact event. *Proceedings of the National Academy of Sciences of the United States of America* 107, 16043–16047.

Dean, J.S., 1978. Independent dating in archaeological analysis. *Advances in Archaeological Method and Theory* 1, 223–255.

Egan, J., Staff, R., Blackford, J., 2015. A high-precision age estimate of the Holocene Plinian eruption of Mount Mazama, Oregon, USA. *The Holocene* 25, 1054–1067.

Firestone, R.B., 2009. The case for the Younger Dryas Extraterrestrial Impact Event: mammoth, megafauna and Clovis extinction. *Journal of Cosmology* 2, 256–285.

Firestone, R.B., West, A., Kennett, J.P., Becker, L., Bunch, T.E., Revay, Z.S., Schultz, P.H., *et al.*, 2007. Evidence for an extraterrestrial impact 12,900 years ago that contributed to the megafaunal extinctions and the Younger Dryas cooling. *Proceedings of the National Academy of Sciences of the United States of America* 104, 16016–16021.

Frechen, J., 1952. Die Herkunft der spätglazialen Bimstuffe in mittel-und süddeutschen Mooren. *Geologisches Jahrbuch* 67, 209–230.

Frechen, J., 1959. Die tuffe des Laacher Vulkangebietes als quartärgeologische Leitgesteine und Zeitmarken. *Fortschritte in der Geologie von Rheinland und Westfalen* 4, 363–370.

Friedrich, W.L., Kromer, B., Friedrich, M., Heinemeier, J., Pfeiffer, T., Talamo, S., 2006. Santorini eruption radiocarbon dated to 1627–1600 B.C. *Science* 312, 548.

Goodyear, A.C., 2013. Update on the 2012–2013 activities of the Southeastern Paleoamerican Survey. *Legacy* 17, 10–12.

Hajic, E.R., Mandel, R.D., Ray, J.H., Lopinot, N.H., 2007. Geoarchaeology of stratified Paleoindian deposits at the Big Eddy Site, Southwest Missouri, U.S.A. *Geoarchaeology* 22, 891–934.

Haynes, C.V., 2007. Radiocarbon dating at Murray Springs and Curry Draw. In: Haynes, C.V., Huckell, B.B. (Eds.), *Murray Springs: A Clovis Site with Multiple Activity Areas in the San Pedro Valley, Arizona*. University of Arizona Press, Tucson, pp. 229–239.

Haynes, C.V., Boerner, J., Domanik, K., Lauretta, D., Ballenger, J., Goreva, J., 2010. The Murray Springs Clovis site, Pleistocene extinction, and the question of extraterrestrial impact. *Proceedings of the National Academy of Sciences of the United States of America* 107, 4010–4015.

Haynes, V., Agogino, G., 1960. *Geological significance of a new radiocarbon date from the Lindenmeier Site*. The Denver Museum of Natural History Proceedings No. 9. The Denver Museum of Natural History, Denver.

Heine, K., 1993. Warmzeitliche Bodenbildung im Bölling/Alleröd im Mittelrheingebiet. *Decheniana* 146, 315–324.

Holliday, V., Surovell, T., Johnson, E., 2016. A blind test of the Younger Dryas Impact Hypothesis. *PLOS One* 11, e0155470. https://doi.org/10.1371/journal.pone.0155470

Holliday, V.T., Meltzer, D.J., 2010. The 12.9-ka ET Impact Hypothesis and North American Paleoindians. *Current Anthropology* 51, 575–607.

International Study Group, 1982. An inter-laboratory comparison of radiocarbon measurements in tree rings. *Nature* 298, 619–623.

Israde-Alcantara, I., Bischoff, J.L., Dominguez-Vazquez, G., Li, H.-C., DeCarli, P.S., Bunch, T.E., Wittke, J.H., *et al.*, 2012. Evidence from central Mexico supporting the Younger Dryas extraterrestrial impact hypothesis. *Proceedings of the National Academy of Sciences of the United States of America* 109, E738–E747.

Kennett, D., Kennett, J., West, G., Erlandson, J., Johnson, J., Hendy, I., West, A., Culleton, B., Jones, T., Staffordjr, T., 2008. Wildfire and abrupt ecosystem disruption on California's Northern Channel Islands at the Ållerød–Younger Dryas boundary (13.0–12.9ka). *Quaternary Science Reviews* 27, 2530–2545.

Kennett, D.J., Kennett, J.P., West, A., Mercer, C., Hee, S.S.Q., Bement, L., Bunch, T.E., Sellers, M., Wolbach, W.S., 2009a. Nanodiamonds in the Younger Dryas boundary sediment layer. *Science* 323, 94–94.

Kennett, D.J., Kennett, J.P., West, A., West, G. J., Bunch, T.E., Culleton, B.J., Erlandson, J.M., Hee, S.S.Q., Johnson, J.R., Mercer, C., 2009b. Shock-synthesized hexagonal diamonds in Younger Dryas boundary sediments. *Proceedings of the National Academy of Sciences of the United States of America* 106, 12623–12628.

https://doi.org/10.1017/qua.2019.83 Published online by Cambridge University Press

Kennett, J.P., Kennett, D.J., Culleton, B.J., Aura Tortosa, J.E., Bischoff, J.L., Bunch, T.E., Daniel, I.R., *et al*., 2015. Bayesian chronological analyses consistent with synchronous age of 12,835–12,735 Cal B.P. for Younger Dryas boundary on four continents. *Proceedings of the National Academy of Sciences of the United States of America* 112, E4344–E4353.

Kinzie, C.R., Que Hee, S.S., Stich, A., Tague, K.A., Mercer, C., Razink, J.J., Kennett, D.J., *et al*., 2014. Nanodiamond-rich layer across three continents consistent with major cosmic impact at 12,800 Cal BP. *Journal of Geology* 122, 475–506.

Kjær, K.H., Larsen, N.K., Binder, T., Bjørk, A.A., Eisen, O., Fahnestock, M.A., Funder, S., *et al*., 2018. A large impact crater beneath Hiawatha Glacier in northwest Greenland. *Science Advances* 4, eaar8173.https://doi.org/10.1126/sciadv.aar8173

Kletetschka, G., Vondrák, D., Hruba, J., Prochazka, V., Nabelek, L., Svitavská-Svobodová, H., Bobek, P., *et al*., 2018. Cosmic-impact event in lake sediments from Central Europe post-dates the Laacher See eruption and marks onset of the Younger Dryas. *Journal of Geology* 126, 561–575.

Kromer, B., Spurk, M., Remmele, S., Barbetti, M., Joniello, V., 1998. Segments of atmospheric ^{14}C change as derived from Late Glacial and Early Holocene floating tree-ring series. *Radiocarbon* 40, 351–358.

LeCompte, M.A., Goodyear, A.C., Demitroff, M.N., Batchelor, D., Vogel, E.K., Mooney, C., Rock, B.N., Seidel, A.W., 2012. Independent evaluation of conflicting microspherule results from different investigations of the Younger Dryas Impact Hypothesis. *Proceedings of the National Academy of Sciences of the United States of America* 109, E2960–E2969.

Lopinot, N.H., Ray, J.H., Conner, M.D., 1998. *The 1997 Excavations at the Big Eddy Site (23CE426) in Southwest Missouri*. Center for Archaeological Research Special Publication No. 2. Report submitted to the United States Army Corps of Engineers, Kansas City District. Southwest Missouri State University, Springfield.

McElreath, R., 2017. rethinking v1.59: Statistical rethinking book package.

Meltzer, D.J., Holliday, V.T., Cannon, M.D., Miller, D.S., 2014. Chronological evidence fails to support claim of an isochronous widespread layer of cosmic impact indicators dated to 12,800 years ago. *Proceedings of the National Academy of Sciences of the United States of America* 111, E2162–E2171.

Moore, C.R., West, A., LeCompte, M.A., Brooks, M.J., Daniel, I.R., Goodyear, A.C., Ferguson, T.A., *et al*., 2017. Widespread platinum anomaly documented at the Younger Dryas onset in North American sedimentary sequences. *Scientific Reports* 7, 44031.

Okuno, M., Shiihara, M., Masayuki, T., Nakamura, T., Han Kim, K., Domitsu, H., Moriwaki, H., Oda, M., 2010. AMS radiocarbon dating of Holocene tephra layers on Ulleung Island, South Korea. *Radiocarbon* 52, 1465–1470.

Paquay, F.S., Goderis, S., Ravizza, G., Vanhaeck, F., Boyd, M., Surovell, T.A., Holliday, V.T., Haynes, C.V., Claeys, P., 2009. Absence of geochemical evidence for an impact event at the Bølling–Allerød/Younger Dryas transition. *Proceedings of the National Academy of Sciences of the United States of America* 106, 21505–21510.

Park, C., Schmincke, H.-U., 1997. Lake formation and catastrophic dam burst during the Late Pleistocene Laacher See eruption (Germany). *Natur Wissenschaften* 84, 521–525.

Parnell, A.C., Haslett, J., Allen, J.R.M., Buck, C.E., Huntley, B., 2008. A flexible approach to assessing synchroneity of past events using Bayesian reconstructions of sedimentation history. *Quaternary Science Reviews* 27, 1872–1885.

Pedersen, T.L., 2018. patchwork v0.0.1: The Composer of ggplots. https://github.com/thomasp85/patchwork, accessed January 10, 2019.

Petaev, M.I., Huang, S., Jacobsen, S.B., Zindler, A., 2013. Large Pt anomaly in the Greenland ice core points to a cataclysm at the onset of Younger Dryas. *Proceedings of the National Academy of Sciences of the United States of America* 110, 12917–12920.

Pigati, J.S., Latorre, C., Rech, J.A., Betancourt, J.L., Martinez, K.E., Budahn, J.R., 2012. Accumulation of impact markers in desert wetlands and implications for the Younger Dryas impact hypothesis. *Proceedings of the National Academy of Sciences of the United States of America* 109, 7208–7212.

Pino, M., Abarzúa, A.M., Astorga, G., Martel-Cea, A., Cossio-Montecinos, N., Navarro, R.X., Paz Lira, M., *et al*., 2019. Sedimentary record from Patagonia, southern Chile supports cosmic-impact triggering of biomass burning, climate change, and megafaunal extinctions at 12.8 ka. *Scientific Reports* 9, 4413.

Pinter, N., Scott, A.C., Daulton, T.L., Podoll, A., Koeberl, C., Anderson, R.S., Ishman, S.E., 2011. The Younger Dryas impact hypothesis: a requiem. *Earth-Science Reviews* 106, 247–264.

Polach, H.A., 1974. Application of liquid scintillation spectrometers to radiocarbon dating. In: Stanley, P.E., Scoggins, B.A. (Eds.), *Liquid Scintillation Counting: Recent Developments*. Academic Press, New York and London, pp. 153–171.

R Core Team, 2018. R: A language and environment for statistical computing. R Foundation for Statistical Computing, Vienna.

Reimer, P.J., Bard, E., Bayliss, A., Beck, J.W., Blackwell, P.G., Ramsey, C.B., Buck, C.E., Cheng, H., Edwards, R.L., Friedrich, M., 2013. IntCal13 and Marine13 radiocarbon age calibration curves 0–50,000 years cal BP. *Radiocarbon* 55, 1869–1887.

Rubin, M., Alexander, C., 1960. U.S. Geological Survey radiocarbon dates V. *Radiocarbon* 2, 129–185.

Schiffer, M.B., 1986. Radiocarbon dating and the "old wood" problem: The case of the Hohokam chronology. *Journal of Archaeological Science* 13, 13–30.

Schmincke, H.-U., Park, C., Harms, E., 1999. Evolution and environmental impacts of the eruption of Laacher See Volcano (Germany) 12,900 a BP. *Quaternary International* 61, 61–72.

Schweitzer, H.-J., 1958. Entstehung und flora des Trasses im nördlichen Laachersee-Gebiet. *E&G Quaternary Science Journal* 9, 28–48.

Scott, A.C., Pinter, N., Collinson, M.E., Hardiman, M., Anderson, R.S., Brain, A.P.R., Smith, S.Y., Marone, F., Stampanoni, M., 2010. Fungus, not comet or catastrophe, accounts for carbonaceous spherules in the Younger Dryas "impact layer": Origin of carbonaceous spherules. *Geophysical Research Letters* 37, L14302. https://doi.org/10.1029/2010GL043345

Scott, E.M., Aitchison, T.C., Harkness, D.D., Cook, G.T., Baxter, M.S., 1990. An overview of all three stages of the International Radiocarbon Intercomparison. *Radiocarbon* 32, 309–319.

Scott, E.M., Cook, G.T., Naysmith, P., 2010a. A report on phase 2 of the Fifth International Radiocarbon Intercomparison (VIRI). *Radiocarbon* 52, 846–858.

Scott, E.M., Cook, G.T., Naysmith, P., 2010b. The Fifth International Radiocarbon Intercomparison (VIRI): An assessment of laboratory performance in stage 3. *Radiocarbon* 52, 859–865.

Scott, E.M., Cook, G.T., Naysmith, P., Bryant, C., O'Donnell, D., 2007. A report on phase 1 of the 5th International Radiocarbon Intercomparison (VIRI). *Radiocarbon* 49, 409–426.

Scott, E.M., Harkness, D.D., Cook, G.T., 1998. Interlaboratory comparisons: Lessons learned. *Radiocarbon* 40, 331–340.

Stan Development Team, 2018. RStan 2.17.2: The R interface for Stan. https://mc-stan.org/, accessed Dec 20, 2017.

Steegen, S., Tuerlinckx, F., Gelman, A., Vanpaemel, W., 2016. Increasing transparency through a multiverse analysis. *Perspectives in Psychological Science* 11, 702–712.

Street, M.J., 1993. Analysis of Late Palaeolithic and Mesolithic Faunal Assemblages in the Northern Rhineland, Germany. PhD dissertation, University of Birmingham, Brimingham, United Kingdom.

Street, M.B., Baales, M., Weninger, B., 1994. Absolute Chronologie des späten Paläolithikums und des Frühmesolithikums im nördlichen Rheinland. *Archäologisches Korrespondenzblatt* 241994, 1–28.

Surovell, T.A., Holliday, V.T., Gingerich, J.A.M., Ketron, C., Haynes, C.V., Hilman, I., Wagner, D.P., Johnson, E., Claeys, P., 2009. An independent evaluation of the Younger Dryas Extraterrestrial Impact Hypothesis. *Proceedings of the National Academy of Sciences of the United States of America* 106, 18155–18158.

Tankersley, K.B., Redmond, B.G., 1999. Radiocarbon dating of a Paleoindian projectile point from Sheriden Cave, Ohio. *Current Research in the Pleistocene* 16, 76–77.

van den Bogaard, P., 1983. Die Eruption des Laacher See Vulkans. PhD dissertation, Ruhr-Universität, Bochum, Germany.

van den Bogaard, P., Schmincke, H.-U., 1985. Laacher See Tephra: A widespread isochronous Late Quaternary tephra layer in central and northern Europe. *Geological Society of America Bulletin* 96, 1554–1571.

van der Hammen, T., van Geel, B., 2008. Charcoal in soils of the Allerød-Younger Dryas transition were the result of natural fires and not necessarily the effect of an extra-terrestrial impact. *Netherlands Journal of Geosciences* 87, 359–361.

van Hoesel, A., Hoek, W.Z., Braadbaart, F., van der Plicht, J., Pennock, G.M., Drury, M.R., 2012. Nanodiamonds and wildfire evidence in the Usselo Horizon postdate the Allerød-Younger Dryas boundary. *Proceedings of the National Academy of Sciences of the United States of America* 109, 7648–7653.

van Hoesel, A., Hoek, W.Z., Pennock, G.M., Drury, M.R., 2014. The Younger Dryas impact hypothesis: A critical review. *Quaternary Science Reviews* 83, 95–114.

Walton, A., Trautman, M.A., Friend, J.P., 1961. Isotopes, Inc. radiocarbon measurements I. *Radiocarbon* 3, 47–59.

Wang, Y., Amundson, R., Trumbore, S., 1996. Radiocarbon dating of soil organic matter. *Quaternary Research* 45, 282–288.

Ward, G.K., Wilson, S.R., 1978. Procedures for comparing and combining radiocarbon age determinations: a critique. *Archaeometry* 20, 19–31.

Waters, M.R., Stafford, T.W., Redmond, B.G., Tankersley, K.B., 2009. The age of the Paleoindian assemblage at Sheriden Cave, Ohio. *American Antiquity* 74, 107–111.

Wickham, H., 2007. Reshaping data with the reshape package. *Journal of Statistical Software* 21, 1–20.

Wickham, H., 2016. ggplot2: Elegant graphics for data analysis. Springer, New York.

Wittke, J.H., Weaver, J.C., Bunch, T.E., Kennett, J.P., Kennett, D.J., Moore, A.M.T., Hillman, G.C., *et al*., 2013. Evidence for deposition of 10 million tonnes of impact spherules across four continents 12,800 y ago. *Proceedings of the National Academy of Sciences USA* 110, E2088–E2097.

Wolbach, W.S., Ballard, J.P., Mayewski, P.A., Adedeji, V., Bunch, T.E., Firestone, R.B., French, T.A., *et al*., 2018a. Extraordinary biomass-burning episode and impact winter triggered by the Younger Dryas cosmic impact ~12,800 Years Ago. 1. Ice cores and glaciers. *Journal of Geology* 126, 165–184.

Wolbach, W.S., Ballard, J.P., Mayewski, P.A., Parnell, A.C., Cahill, N., Adedeji, V., Bunch, T.E., *et al*., 2018b. Extraordinary biomass-burning episode and impact winter triggered by the Younger Dryas cosmic impact ~12,800 Years Ago. 2. Lake, marine, and terrestrial sediments. *Journal of Geology* 126, 185–205.

Wu, Y., Sharma, M., LeCompte, M.A., Demitroff, M.N., Landis, J.D., 2013. Origin and provenance of spherules and magnetic grains at the Younger Dryas boundary. *Proceedings of the National Academy of Sciences of the United States of America* 110, E3557–E3566.

https://doi.org/10.1017/qua.2019.83 Published online by Cambridge University Press